

Investigations on the cell metabolomics basis of multidrug resistance from tumor cells by ultra-performance liquid chromatography–mass spectrometry

Ruixing Zhang^{1,2} · Xiaoyu Zhuang^{1,2} · Li Zong^{1,2} · Shu Liu¹ · Zhiqiang Liu¹ · Fengrui Song¹

Received: 6 April 2016 / Revised: 2 June 2016 / Accepted: 6 June 2016 / Published online: 5 July 2016
© Springer-Verlag Berlin Heidelberg 2016

Abstract Although anticancer drug resistance has been linked to high expression of P-glycoprotein and the enhanced DNA repair ability, the biochemical process and the underlying mechanisms of drug resistance are not clear. In order to clarify the biochemical mechanisms of drug resistance during anticancer drug treatment, we studied the metabolomics of MCF-7/S and MCF-7/Adr cell lines, the COC1 and COC1/DDP cell lines, including the metabolic pathways of multidrug-resistant tumor cells and the changes of endogenous substances in cells. The intracellular metabolites were profiled using ultra-performance liquid chromatography–tandem mass spectrometry (UPLC–MS/MS). In this study, 24 biomarkers in MCF-7/Adr cells and 15 biomarkers in COC1/DDP cells that are involved in some important metabolic pathways were putatively identified. Several metabolic pathways are changed in tumor cells showing drug resistance, such as protein synthesis pathways, cysteine synthesis, the glutamine metabolic pathway, and the ammonia cycle; the first of these are involved in the synthesis of some important proteins including membrane proteins, multidrug resistance-associated proteins, and P-glycoprotein (P-gp). Proteins related to drug resistance were overexpressed in multidrug-

resistant tumor cells. These proteins depended on energy and play important roles in the emergence of drug resistance. The changes in glutathione and cysteine metabolic pathways showed that the cells can activate related metabolic pathways and reduce the cell apoptosis when they encounter oxidative damage. These findings indicate that drug resistance is likely associated with increased P-gp synthesis and reduced apoptosis of tumor cells.

Keywords Ultra-performance liquid chromatography–mass spectrometry · Multidrug resistance · Cell metabolomics · Tumor

Introduction

Doxorubicin is a popular DNA-intercalating agent for breast cancer therapy [1, 2]. Its anticancer mechanisms are well known, including direct intercalation between DNA bases, DNA strand breaks [3], free oxygen radical generation, increased lipid peroxidation, membrane structure alterations, and the effects on apoptosis pathways through caspase-3 activation and p21 induction [4, 5]. However, breast cancer patients often encounter drug resistance during continuous dosing of doxorubicin, which poses a great challenge to using doxorubicin in breast cancer treatment [6]. This situation also occurred with cisplatin.

The popular MCF-7 breast cancer cell line can produce a stable and resistant cell line, MCF-7/Adr, which is resistant to doxorubicin after chronic exposure to doxorubicin to sensitive breast cancer cell lines [7]. COC1/DPP as well as MCF-7/Adr, which is resistant to cisplatin, was also produced by chronic exposure to cisplatin.

By using genomics and proteomics methods, researchers have investigated the mechanisms of drug resistance induced

Ruixing Zhang and Xiaoyu Zhuang contributed equally to this work.

✉ Fengrui Song
songfr@ciac.ac.cn

¹ National Center of Mass Spectrometry in Changchun, Jilin Province Key Laboratory of Chinese Medicine Chemistry and Mass Spectrometry, Changchun Institute of Applied Chemistry, Chinese Academy of Sciences, 5625 Renmin Street, Changchun, Jilin 130022, China

² University of the Chinese Academy of Sciences, Beijing 100039, China

by doxorubicin or cisplatin [8]. The results revealed that some genes [9, 10] and proteins are related to drug resistance [11, 12]. Some cell factors also play important roles in the development of drug resistance, e.g., epithelial-to-mesenchymal transition as well as altered heat shock response elements [13]. Proteomics comparing analyses between drug-resistant and drug-sensitive MCF-7 cells identified that several proteins involved in apoptosis, the cell cycle, glucose metabolism, and fatty acid oxidation contribute to drug resistance [14]. The genomic analysis of drug-resistant cell lines revealed that the drug resistance is related to gene repair [15], cell cycle regulation, and overexpression of multidrug-resistant genes [16]. Although the resistance-related genes and proteins have been investigated and several metabolic pathways involved in MCF-7/Adr drug resistance have been found [17], little is known about the global metabolic pattern and shift between the sensitive and resistant breast tumor cells.

Although tumor cells were characterized by reprogrammed metabolic pathways including enhanced anaerobic glycolysis and reduced tricarboxylic acid cycle (TCA) activity [18], i.e., the Warburg effect [19], alternative utilization of glutamine as an energy supply, and the glycine in rapid tumor cell proliferation [20], the metabolomics characteristics of drug-resistant tumor cells are not well understood [5, 21].

Metabolomics is a quantitative measurement of the dynamic metabolic response of living systems to genetic modifications, physiological and environment changes, and so forth [22]. Metabolomics used for the high-throughput analysis of low molecular mass compounds in cells or biological samples [23] reflects the metabolic shifts involved in biological processes; thus, it might reveal the underlying mechanisms involved in these processes [24]. Studies of the effects of chemotherapeutic agents on drug-resistant MCF-7/Adr cells would provide useful information to understand the mechanisms of drug resistance.

In this study, metabolomics was employed to profile intracellular metabolites in MCF-7/Adr and MCF-7/S cells. Some potential biomarkers were identified and the metabolic pathways were analyzed to illustrate the mechanisms of drug resistance in the cellular metabolic processes. Metabolic patterns and potential markers identified can be used for evaluating the pharmacodynamics and exploring the mechanisms of tumor cells resistant to doxorubicin.

Experimental

Materials

Doxorubicin and cisplatin were purchased from Hisun Pharm Co. (Taizhou, China). Ethanol, acetonitrile, and chloroform (HPLC grade) were purchased from Dima Co. Water used as the HPLC mobile phase was deionized with an Alpha-Q

purifier from Millipore (Bedford, USA). MCF-7/S and MCF-7/Adr were obtained from Chinese Academy of Medical Science (the 57th generation; MCF-7/S and MCF-7/Adr were in the same generation). RPMI-1640 medium was obtained from Hyclone, China. Fetal bovine serum was supplied by Hangzhou Sijiqing Co Ltd. Penicillin and streptomycin were purchased from Beijing Dingguo Co. Ltd. The GENiosPro plate reader was purchased from Tecan (Switzerland).

Cell culture

Human MCF-7 breast cancer cells and the doxorubicin-resistant subline (MCF-7/Adr) were grown in RPMI-1640 medium supplemented with 10 % (v/v) fetal bovine serum. COC1 and COC1/DDP cells were cultured in DMEM medium with 100 U/ml penicillin and 0.1 mg/ml streptomycin at 37 °C with 5 % CO₂. Both cell lines were cultured in six-well plates and grown to nearly 90 % confluence. MCF-7/Adr cells were incubated with 10 μM doxorubicin for 48 h and then changed to fresh medium without doxorubicin. After another 24 h, the culture medium in each well was collected, and the residues were discarded. The adherent cells were washed twice with PBS immediately before adding 300 μL of trypsin solutions (5 %) to each well. Cells were then collected into 1.5-mL tubes (three replicates were cultured in parallel and the mean of these was obtained).

Cell viability assays

To monitor the cell viability during the stimulations of apoptosis and necrosis, the MTT assay was performed. Cells were grown in 96-well plates. After 24 h, 10 mL of 5 mg/ml solution of MTT (Roche, Indianapolis, IN, USA) in PBS buffer was added to each well and the cells were incubated at 37 °C for 4 h. The medium was then completely removed. To each well, 100 μL of DMSO was added and the plates were incubated for 40 min at room temperature. Optical absorbance of reduced MTT, reflecting the viability of the cells, was measured at 590 nm using a GENiosPro plate reader [25].

Sample preparation

The metabolites from MCF-7/S and MCF-7/Adr cells were obtained as described in elsewhere [10]. Briefly, at the end of the incubation periods, the cells were washed rapidly with precooled PBS and then treated with trypsin. Each digested sample was resuspended in 150 μL of sterilized ultrapure water. The resulting solution was frozen for 10 min in a freezer at -80 °C and then put into a 37 °C water bath; this process was repeated three times. *N,N*-Dimethyl-L-phenylalanine (N, N-Phe) was spiked to correct the retention time. Cell lysates were added with 600 μL ice methanol and the mixture was

then vortexed for 5 min. Thereafter, 400 μL chloroform was added into the sample tube to extract the metabolites, and the mixture was vortexed for 5 min. The sample tube was then stored at $-20\text{ }^{\circ}\text{C}$ for 6–8 h. After the tube was centrifuged at 12,000 rpm for 5 min at $4\text{ }^{\circ}\text{C}$, the supernatant was transferred to a filter cap and centrifuged again at 12,000 rpm for 5 min at $4\text{ }^{\circ}\text{C}$. The filtrate was collected and freeze-dried by nitrogen.

UPLC–MS and UPLC–MS/MS analysis

The UPLC–MS and UPLC–MS/MS experiments were performed with a Waters Acquity™ ultra-performance liquid chromatography system coupled with a Waters Synapt G2 Q-TOF mass spectrometer (Waters, Manchester, UK). Chromatographic separation was carried out at $25\text{ }^{\circ}\text{C}$ on an ACQUITY UPLC HSS T3 column ($2.1\text{ mm} \times 100\text{ mm}$, $1.7\text{ }\mu\text{M}$, Waters). The mobile phase consisted of A (0.1 % formic acid in water) and B (0.1 % formic acid in acetonitrile). The optimized UPLC elution conditions were as follows: 0–1.0 min, 10 % B; 1.0–4.0 min, 10–36 % B; 4.0–7.0 min, 36–85 % B; 7.0–10.0 min, 85–100 % B; 10.0–16.0 min, 100 % B; 16.0–16.1 min, 100.0–10.0 % B; and 16.1–20.0 min, 10.0 % B. The flow rate was 0.5 mL/min. The autosampler was maintained at $4\text{ }^{\circ}\text{C}$. A sample volume of 5 μL was injected for each run.

The MS conditions are as follows: the m/z scan range was from 50 to 1200. In negative ion mode, the capillary and cone voltage were set at -2.5 kV and 45 V , respectively. In positive ion mode, the capillary and cone voltage were set at 3.0 kV and 45 V , respectively. The desolvation gas was set to 600 L/h at a temperature of $400\text{ }^{\circ}\text{C}$, the cone gas was set to 30 L/h, and the source temperature was set to $120\text{ }^{\circ}\text{C}$. The data acquisition rate was set to 0.1 s, with a 0.1-s interscan delay. The MS^E experiment with two scan functions was carried out with the following parameters: function 1: m/z 50–1200, 0.1 s scan duration, 0.02 s interscan delay, collision energy ramp of 10–30 V; function 2: m/z 50–1200, 0.1 s scan duration, 0.02 s interscan delay, collision energy ramp of 10–20 V. MS^E mode enabled almost simultaneous acquisition of both MS and MS/MS data in a single analytical run. All analyses were acquired using the lock spray to ensure accuracy and reproducibility. Leucine–enkephalin was used as the lock mass at a concentration of 300 ng/ml and flow rate of 5 $\mu\text{L}/\text{min}$. Data were collected in continuum mode, the lock spray frequency was set at 10 s, and data were averaged over 10 scans. All the acquisition and analysis of data were controlled by Waters MassLynx v 4.1 software [26].

Quantification of metabolites was performed using LC–MS/MS where a liquid chromatograph is coupled with a triple quadrupole mass spectrometer (Xevo-TQ, Waters). All the acquisition data were analyzed by masslynx 4.1 software.

Data treatment and statistical analysis

The mass data acquired were imported to Markerlynx XS (Waters Corp., Milford, MA, USA) within the Masslynx software for peak detection and alignment. Prior to analysis, the quality of the resulting data should be checked in the metabolic fingerprinting assay. The raw data obtained from UPLC–Q-TOF-MS was converted into network common data using the Masslynx software (Waters Corp, Milford, MA).

For comparison, data were filtered by choosing only the features that were present in all samples in one of the compared groups. To approximate a normal distribution, data were scaled by applying the common logarithm to the abundances after filtering.

Markerlynx XS software was used to preprocess the UPLC–Q-TOF-MS data using several algorithms including the filtration and the normalization. For filtration and detection of ion peaks, the ion chromatograms were extracted by using relative model peaks. The UPLC–Q-TOF-MS data were cut into slices by a peak detection algorithm based on mass unit, and then the retention time in the total ion chromatograph was recorded. The retention time and relative intensity were compared to generate the mass domain bins in which to group peaks. UPLC–Q-TOF-MS data on the retention time and the peak intensity, i.e., in two dimensions, was analyzed by Markerlynx XS Microsoft. The drift retention time was corrected and the peak intensity was compared from run to run. For each group, the median value and the deviation of retention time for each mass unit in that group were calculated.

SIMCA-P software (V11.5, Umetrics, Umea, Sweden) was used to conduct orthogonal partial least-squares discriminant analysis (OPLS-DA) in which the OPLS model comprises two blocks of modeled variation, i.e., the Y predictive (T_p) block refers to the class variation and the Y orthogonal (T_o) block refers to the uncorrelated variation. The score plots for t_p and t_o afforded a visual classification of MCF-7/Adr and MCF-7/S. After we obtained the score plot, the data was analyzed by the OPLS-DA model and then the loading plot, which had an S shape. The metabolites that far from the origin were chosen to create a marker list. In this list, the variable importance in the projection (VIP) value and p value were clear.

The differences among samples were evaluated for individual metabolites by using an independent samples t test ($p < 0.05$) and a VIP value generated by SIMCA-P in the OPLS-DA model of more than 1.0. These metabolites were chosen as potential biomarkers, and the accurate mass of features representing significant differences was searched against METLIN, mass Trix public databases, Madison Metabolomics Consortium Database (MMCD), and Human Metabolite Database (HMDB). To identify the metabolite more accurately, the mass accuracy was set at 30 ppm.

Results and discussion

Persistent resistance of MCF-7/Adr cells to doxorubicin

Drug-resistant cell lines are usually generated from drug-sensitive cells by maintaining a low concentration of drug in the cells and gradually increasing the dose over time. The drug-resistant cell line of MCF-7/Adr is characterized by overexpression of P-glycoprotein and the failure of DNA repair which leads to gene mutation. For the gene mutation the drug's target is also changed. In this paper, MCF-7/S and MCF-7/Adr cells were maintained in RPMI-1640 medium only supplemented with 10 % (v/v) FBS, and then the effect of different concentrations of doxorubicin on cell viability was examined by the MTT method to verify whether the insensitivity of MCF-7/Adr cells to doxorubicin was persistent and whether they exhibited high tolerance to doxorubicin. As expected, the MCF-7/Adr cells showed higher survival rates compared to MCF-7/S cells after being maintained in doxorubicin culture medium (Fig. 1).

Optimization of experimental conditions

The extracts of cells were measured both in positive and negative ion ESI modes in to optimize the experimental conditions. More metabolites with lower noise level and matrix effects were detected using positive ion ESI. A 20-min UPLC gradient program was employed to separate the metabolites (see "UPLC-MS and UPLC-MS/MS analysis"). The autosampler compartment was set at 4 °C throughout the analysis to minimize thermal

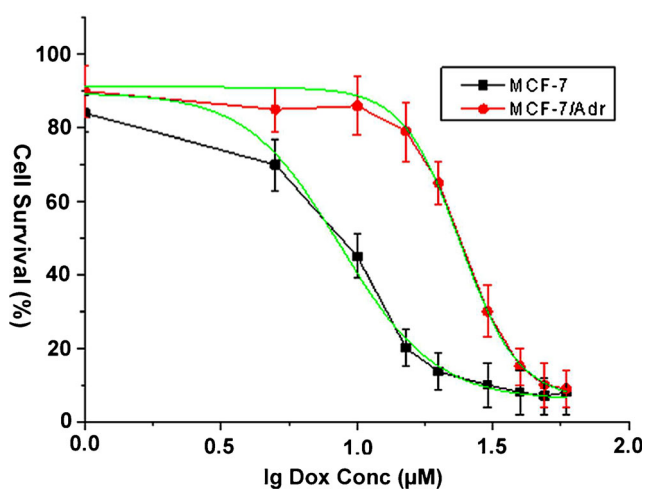


Fig. 1 Sensitivity of MCF-7/S and MCF-7/Adr cells to doxorubicin treatment. (As the MTT results show, the IC_{50} values for doxorubicin against the MCF-7 and MCF-7/Adr cell lines were 0.8 μ M and 1.4 μ M, respectively)

degradation of the metabolites. As shown in Fig. 2a, a good number of metabolites were eluted and detected within 18 min with better separation.

Data analysis

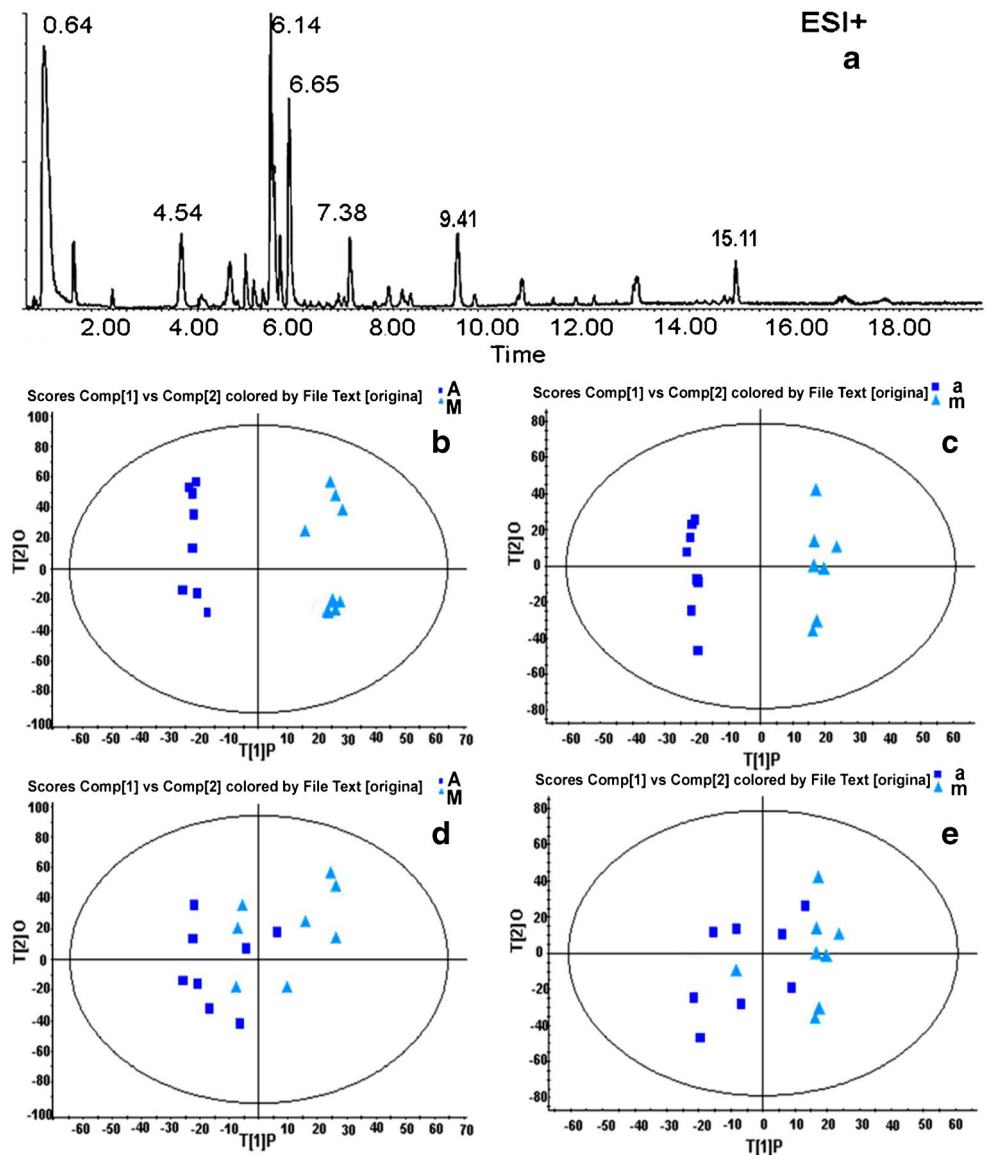
The cancer cells produced lots of metabolites. The total ion chromatography in positive mode in Fig. 2a shows that many endogenous metabolites were obtained. Figures 2b and c show that the MCF-7/S group and MCF-7/Adr group were distinguished efficiently, indicating a lot of different endogenous metabolites between these groups. We used the SIMCA-P software to find the biomarkers that were far away from the origin on the basis of the loading plot, which was obtained from SIMCA-P. The compounds that had changed dramatically were identified as potential biomarkers. A different significance *t* test was used in this paper ($p < 0.05$). Further identification of the biomarkers was based on LC-MS/MS and the mass spectrometry database search. To explain the metabolic changes of drug-resistant cells, we also compared the metabolites between MCF-7/Adr cells and MCF-7/S cells which were cultured in the medium without doxorubicin. As show in Fig. 2d, e, the metabolites were not changed dramatically.

Metabolite identification

In this study, METLIN, MMCD, and HMDB were used for mass-based metabolite identification. METLIN is a Web-based database that can facilitate the identification of metabolites by using accurate mass data. It includes an annotated list of structural information for known metabolites. The database has links to other public databases such as the Kyoto Encyclopedia of Genes and Genomes (KEGG) and PubChem. Further MS/MS data were obtained for metabolite identification (Fig. 3). For example, the ion at m/z 308.09 with a corresponding compound elution time of 5.76 min was initially assigned as glutathione through a database search, and its identity was further confirmed by MS/MS with the daughter ions at m/z 233.0610, 179.0501, 162.0235, and 76.0129. In total, 24 compounds were putatively identified (Table 1), and these compounds belong to different metabolic pathways. Most of them are related to energy and amino acid metabolism activities that are closely related to drug resistance development [19, 20].

To verify the changes of metabolites, we quantified the concentrations of several important metabolites by triple quadrupole mass spectrometry using the standard and calculated the accurate concentration by calibration curves. The analytical conditions are shown in Table 2. The concentrations of some important metabolites

Fig. 2 Total ion chromatography of metabolites and OPLS-DA score plots. **a** Total ion chromatography of metabolites. Score plot of MCF-7/S and MCF-7/Adr cultured doxorubicin in **b** positive ion mode and **c** negative ion mode. Score plot of MCF-7/S and MCF-7/Adr cultured without doxorubicin in **d** positive ion mode and **e** negative ion model. Squares MCF-7/Adr, triangles MCF-7/S



changed dramatically (Fig. 4). For example, some amino acids, ketoglutarate, NADH, glutathione, and creatine were upregulated dramatically, and L-cysteine and tyrosine were downregulated. These amino acids are related to protein synthesis; ketoglutarate and NADH are related to the energy metabolism; glutathione may be associated with the antioxidant activity. (The result was the mean of three repeats of each cell line).

As shown in Fig. 5, the metabolism of MCF-7/Adr cells changed dramatically. Some secondary metabolites related to energy metabolism and the ammonia cycle, such as pyruvic acid and spermine, increased in MCF-7/Adr cells. But some of the amino acids were reduced in MCF-7/Adr cells, which might be the result of high-speed protein synthesis [13].

To study the common mechanism of drug resistance, we also identified the different metabolites between COC1 cells and COC1/DDP cells which are resistant to cisplatin; the method used to identify the compounds was similar to before. The compounds which have metabolic significance are listed in Table 3. We putatively identified 15 compounds as the most different metabolites by LC-MS/MS. Most of these compounds were similar to the metabolites found in MCF-7/Adr cells.

Table 3 shows that there were some similar metabolites between doxorubicin-resistant cells and cisplatin-resistant cells. These metabolites were amino acids, energy metabolites, or cofactors. Most of the amino acids are related to the biosynthesis of proteins. The glutamine, α -ketoglutarate, and NADH are related to glucose

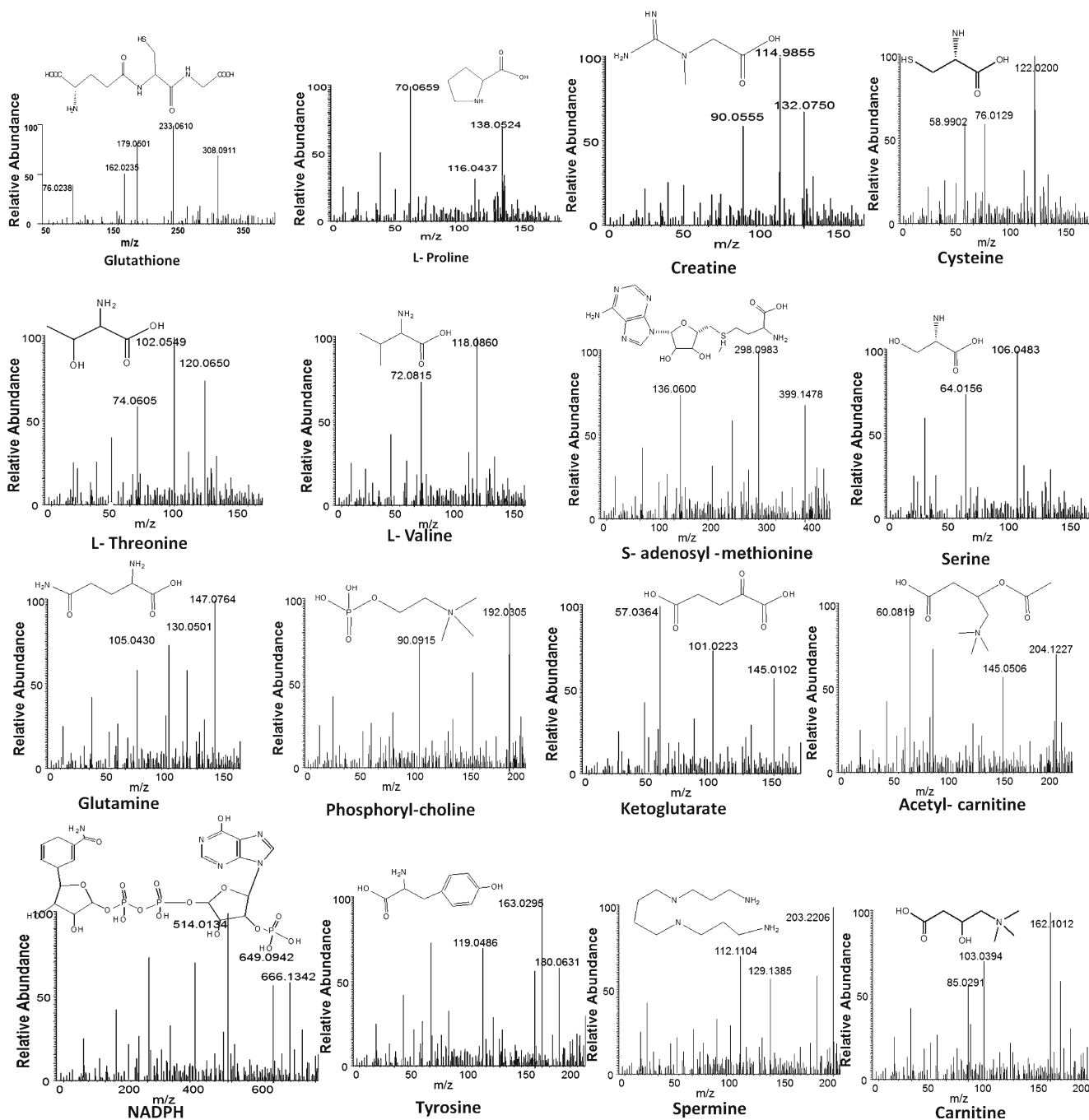


Fig. 3 MS/MS spectra of the endogenous metabolites

metabolites. They are important metabolites for cell proliferation and survival. Metabolites were analyzed by MATELAB 7.0 and the resultant heat map clearly shows the changes of metabolites (Fig. 5).

In this study, the data were input into a Web analysis databank (<http://www.metaboanalyst.ca/faces/ModuleView.xhtml>) and the metabolic pathways were analyzed to find which are largely involved. As shown in Fig. 6, the biosynthesis of amino acyl-tRNA was enhanced the most, reflecting that the biosyntheses of proteins were

enriched including enzymes, transport proteins, and other membrane proteins. Several metabolic pathways related to energy metabolism were also enhanced, including phenylalanine metabolism, pantothenate and CoA biosynthesis, butanoate metabolism, and the citrate cycle. In addition, reactions related to the urine cycle and sulfur transfer, such as arginine, proline, cysteine, and methionine metabolism, were also enhanced. These metabolic pathways might directly or indirectly reflect the drug resistance of tumor cells.

Table 1 Metabolites with significant differences between MCF-7/S cells and MCF-7/Adr cells

| No. | t_R | m/z | Selected ion | Potential result | Elements | P value | VIP value | Fold change | Mass error (ppm) | MS/MS |
|-----|-------|----------|--------------|-----------------------|----------------------------|-----------|-----------|-------------|------------------|---|
| 1 | 1.14 | 138.0524 | $[M + Na]^+$ | L-Proline | $C_5H_9NO_2$ | 0.0039 | 3.02 | +2.3 | -5 | 70.0659 |
| 2 | 0.39 | 102.0317 | $[M + H]^+$ | Acetoacetic acid | $C_4H_6O_3$ | 0.0120 | 1.6 | +1.5 | +1 | 85.0253 70.0084 56.9647 |
| 3 | 2.17 | 90.0711 | $[M + H]^+$ | Beta-Alanine | $C_3H_7NO_2$ | 0.0011 | 6.39 | +1.6 | +17 | 44.0497 |
| 4 | 5.76 | 308.0911 | $[M + H]^+$ | Glutathione | $C_{10}H_{17}N_3O_6S$ | 0.0001 | 4.02 | +5.2 | -2 | 233.0610 179.0501 162.0235 76.0238 |
| 5 | 4.08 | 132.0750 | $[M + H]^+$ | Creatine | $C_4H_9N_3O_2$ | 0.0023 | 1.35 | +4.7 | +17 | 114.9855 90.0555 |
| 6 | 0.89 | 104.0700 | $[M + H]^+$ | Dimethyl-glycine | $C_4H_9NO_2$ | 0.0041 | 5.67 | +3.1 | -10 | 58.0661 |
| 7 | 0.19 | 115.0036 | $[M - H]^-$ | Fumaric acid | $C_4H_6O_4$ | 0.0120 | 1.35 | +2.7 | +5 | 71.0142 |
| 8 | 1.15 | 122.0200 | $[M + H]^+$ | L-Cysteine | $C_3H_7NO_2S$ | 0.0269 | 3.67 | -1.4 | +5 | 58.9902 76.0129 |
| 9 | 3.25 | 132.0952 | $[M + H]^+$ | L-Isoleucine | $C_6H_{13}NO_2$ | 0.0325 | 3.65 | +1.3 | -19 | 86.0969 |
| 10 | 3.19 | 106.0483 | $[M + H]^+$ | L-Serine | $C_3H_7NO_3$ | 0.0098 | 4.35 | -3.1 | -9 | 64.0156 |
| 11 | 1.68 | 120.0650 | $[M + H]^+$ | L-Threonine | $C_4H_9NO_3$ | 0.0059 | 5.21 | -1.4 | -7 | 102.0549 74.0605 56.0500 |
| 12 | 1.13 | 118.0860 | $[M + H]^+$ | L-Valine | $C_5H_{11}NO_2$ | 0.0255 | 1.79 | -1.3 | -7 | 72.0815 |
| 13 | 0.25 | 87.0054 | $[M - H]^-$ | Pyruvic acid | $C_3H_4O_3$ | 0.0321 | 1.32 | +1.1 | -12 | 43.0415 |
| 14 | 0.24 | 90.0550 | $[M + H]^+$ | Sarcosine | $C_3H_7NO_2$ | 0.0055 | 6.31 | +1.2 | -6 | 59.0131 |
| 15 | 11.85 | 399.1478 | $[M + H]^+$ | S-Adenosyl methionine | $C_{15}H_{22}N_6O_5S$ | 0.0054 | 5.32 | +2.7 | +7 | 298.0938 250.0909 136.0600 |
| 16 | 3.36 | 147.0764 | $[M + H]^+$ | Glutamine | $C_5H_{10}N_2O_3$ | 0.0310 | 1.78 | +1.8 | -4 | 130.0501 105.0430 64.0170 |
| 17 | 3.35 | 192.0305 | $[M + Na]^+$ | Phosphorylcholine | $C_4H_{12}NO_4P$ | 0.0098 | 1.29 | +2.6 | -15 | 90.0915 |
| 18 | 0.21 | 145.0102 | $[M - H]^-$ | Ketoglutarate | $C_5H_6O_5$ | 0.0100 | 3.21 | +4.3 | -24 | 101.0223 57.0364 |
| 19 | 2.15 | 184.9816 | $[M - H]^-$ | Phosphoglycerate | $C_3H_7O_7P$ | 0.0044 | 6.32 | -2.1 | +19 | 96.9676 78.9587 |
| 20 | 3.79 | 204.1227 | $[M + H]^+$ | Acetyl carnitine | $C_9H_{17}NO_4$ | 0.0244 | 4.56 | +4.3 | -4 | 145.0506 85.0280 60.0819 |
| 21 | 12.39 | 666.1342 | $[M + H]^+$ | NADH | $C_{21}H_{29}N_7O_{14}P_2$ | 0.0047 | 3.65 | +2.1 | -3 | 649.0942 514.0134 |
| 22 | 2.75 | 180.0631 | $[M - H]^-$ | Tyrosine | $C_9H_{11}NO_3$ | 0.0010 | 2.43 | -3.8 | -2 | 163.0295 119.0486 |
| 23 | 0.24 | 203.2206 | $[M + H]^+$ | Spermine | $C_{10}H_{26}N_4$ | 0.0040 | 6.54 | +4.5 | -15 | 129.1385 112.1104 |
| 24 | 0.39 | 162.1012 | $[M + H]^+$ | Carnitine | $C_7H_{15}NO_3$ | 0.0201 | 2.11 | +1.8 | -12 | 103.0394 85.0291 60.0817 |

Table 2 MS conditions for analysis of the metabolites

| Metabolite | Parents ion | Daughter ion | DP | CE |
|------------------|-------------|--------------|----|----|
| Creatine | 132.08 | 114.99 | 40 | 25 |
| Proline | 138.05 | 70.07 | 34 | 30 |
| Glutathione | 308.09 | 76.02 | 40 | 34 |
| Glutamine | 147.08 | 64.02 | 34 | 32 |
| Glutamate | 148.08 | 64.02 | 34 | 34 |
| Serine | 106.05 | 64.01 | 26 | 24 |
| Ornithine | 133.02 | 70.08 | 34 | 32 |
| Tyrosine | 182.02 | 136.01 | 24 | 24 |
| Carnitine | 162.10 | 103.04 | 28 | 24 |
| SAM | 399.15 | 136.06 | 45 | 37 |
| Ketoglutarate | 145.01 | 101.02 | 28 | 28 |
| NADPH | 666.13 | 649.09 | 48 | 40 |
| Acetyl carnitine | 204.13 | 60.08 | 22 | 18 |
| Sarcosine | 90.05 | 59.01 | 24 | 22 |

In the study of the metabolic difference between COC1 and the cisplatin-resistant cell line COC1/DDP, similar metabolic pathways changed. The enrichment of the biosynthesis of amino acyl-tRNA might reflect the enrichment of protein biosynthesis; the pantothenate and CoA biosynthesis might reflect the glucose metabolism (Fig. 7).

In this study, the intracellular metabolites of MCF-7/Adr or COC1/DDP cells dynamically changed within a few hours after drug treatment. In particular, several amino acids including proline, glutamate, and others or some related metabolic intermediates were dramatically

Fig. 4 Concentration changes of relative metabolites in MCF-7/S cells and MCF-7/Adr cells. (Column are the concentrations of metabolites and error bars are SD values of 3 repeats)

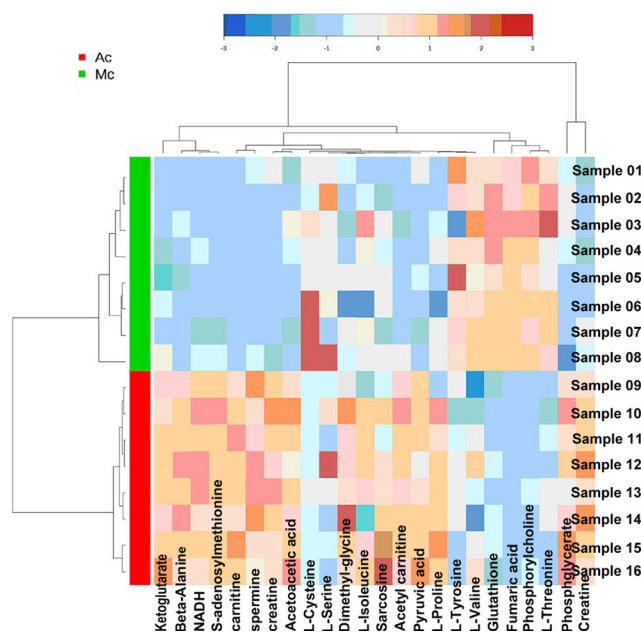
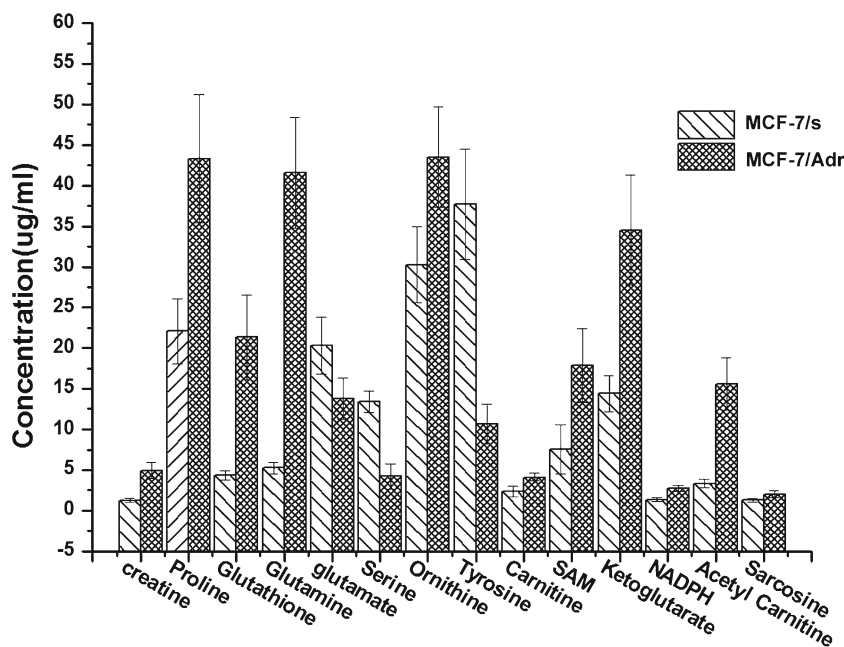


Fig. 5 Hierarchically clustered heat map of metabolism levels in MCF-7/Adr cells and MCF-7/S cells. Rows represent different cell lines, columns represent different reactions. Different color represents the concentration differences of different reactions, e.g., red represents a high concentration and blue represents a low concentration. Red band MCF-7/Adr, green band MCF-7/S

upregulated or downregulated. They were continuously altered in MCF-7/Adr cells after doxorubicin treatment.

Energy is a primary requirement for life as every process needs energy [27]. In this study, we found that more energy and related substances are needed by the drug-resistant cells (Fig. 8). 3-Phosphoglycerate as a biochemically significant 3-

Table 3 Metabolites with significant differences between COC1 cells and COC1/DDP cells

| No. | t_R | m/z | Selected ion | Potential result | Elements | P value | VIP value | Fold change | Mass error (ppm) | MS/MS |
|-----|-------|----------|----------------------|-----------------------|---|-----------|-----------|-------------|------------------|---|
| 1 | 3.10 | 132.0938 | [M + H] ⁺ | L-Leucine | C ₆ H ₁₃ NO ₂ | 0.0325 | 3.70 | +3.3 | -29 | 86.0990 |
| 2 | 9.41 | 150.0589 | [M + H] ⁺ | L-Methionine | C ₃ H ₇ NO ₃ | 0.0058 | 4.35 | -5.4 | +8 | 134.0279 |
| 3 | 1.15 | 122.0180 | [M + H] ⁺ | L-Cysteine | C ₃ H ₇ NO ₂ S | 0.0269 | 3.96 | -4.4 | -8 | 58.9892 76.0129 |
| 4 | 1.13 | 118.0860 | [M + H] ⁺ | L-Valine | C ₅ H ₁₁ NO ₂ | 0.0255 | 1.79 | -2.1 | -1 | 72.0815 |
| 5 | 1.68 | 120.0650 | [M + H] ⁺ | L-Threonine | C ₄ H ₉ NO ₃ | 0.0059 | 5.21 | -1.4 | -9 | 102.0549 74.0605 |
| 6 | 5.76 | 308.0905 | [M + H] ⁺ | Glutathione | C ₁₀ H ₁₇ N ₃ O ₆ S | 0.0002 | 3.00 | +4.2 | -4 | 233.0610 179.0501 162.0235 76.0238 |
| 7 | 0.25 | 87.0059 | [M - H] ⁻ | Pyruvic acid | C ₃ H ₄ O ₃ | 0.0326 | 1.33 | +2.1 | -26 | 43.0415 |
| 8 | 0.24 | 90.0561 | [M + H] ⁺ | Sarcosine | C ₃ H ₇ NO ₂ | 0.0057 | 6.37 | +1.2 | +7 | 59.0131 |
| 9 | 11.85 | 399.1481 | [M + H] ⁺ | S-Adenosyl methionine | C ₁₅ H ₂₂ N ₆ O ₅ S | 0.0055 | 5.33 | +7.7 | +8 | 298.0938 250.0909 136.0600 |
| 10 | 3.36 | 147.0759 | [M + H] ⁺ | Glutamine | C ₅ H ₁₀ N ₂ O ₃ | 0.0323 | 2.78 | +2.8 | -7 | 130.0501 105.0430 64.0170 |
| 11 | 0.21 | 145.0110 | [M - H] ⁻ | α-Ketoglutarate | C ₅ H ₆ O ₅ | 0.0150 | 3.26 | +3.3 | -19 | 101.0223 57.0364 |
| 12 | 12.39 | 666.1326 | [M + H] ⁺ | NADH | C ₂₁ H ₂₉ N ₇ O ₁₄ P ₂ | 0.0044 | 3.60 | +3.6 | +1 | 649.0942 514.0134 |
| 13 | 0.24 | 203.2201 | [M + H] ⁺ | Spermine | C ₁₀ H ₂₆ N ₄ | 0.0040 | 6.55 | +7.5 | -17 | 129.1385 112.1104 |
| 14 | 3.79 | 204.1222 | [M + H] ⁺ | Acetyl carnitine | C ₉ H ₁₇ NO ₄ | 0.0248 | 4.57 | +3.4 | -7 | 145.0506 85.0280 60.0819 |
| 15 | 0.39 | 162.1012 | [M + H] ⁺ | Carnitine | C ₇ H ₁₅ NO ₃ | 0.0201 | 2.11 | +2.4 | -7 | 103.0394 85.0291 60.0817 |

carbon metabolic intermediate in glycolysis. The content changes of 3-phosphoglyceric acid could reflect the changes of energy metabolism in tumor cells. L-Carnitine is a quaternary ammonium compound biosynthesized from the amino acids lysine and methionine. Glutamate and glutamine are important substances during energy metabolism processes. They can interconvert to each other. Glutamate is a key compound in cellular metabolism. It can enter TCA cycle through alpha-ketoglutarate to fuel the TCA cycle and is an important carbon and nitrogen source. Glutamine can be converted into glutamate to provide the source for biomass synthesis.

It was shown that drug-resistant cancer cells were dependent on arginine for optimal growth [28]. When arginine was replaced with ornithine, a urea cycle intermediate and precursor of polyamine synthesis, the arginine failed to restore

growth to the same level. Arginine was also a substrate of nitric oxide synthesis; elevated NO upregulated HIF-1 that is related to signaling transduction pathways [29, 30].

Polyamine was an important factor of microbial growth which was firstly studied in 1958 and can promote growth of *Haemophilus parainfluenzae* [31]. Polyamine was also reported to play a key role in the prevention of nerve damage and duodenal mucosal repair [32]. Spermine was recommended for the treatment of human prostate cancer in individual use or in combination with other anticancer drugs [33]. One report indicates that polyamines can function as growth factors, antioxidants, and stabilizers of DNA, RNA, membranes, metabolic regulators, nutrients as well as secondary messengers [34]. In addition, spermidine and spermine have been shown to bind to the phosphate backbone of polynucleic acids [35].

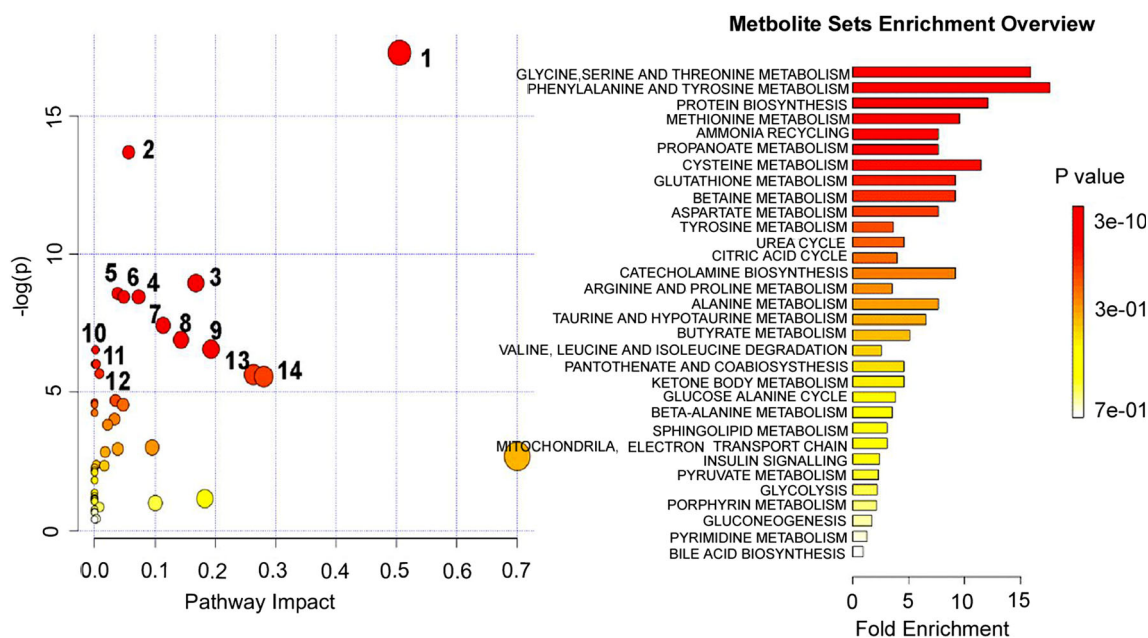


Fig. 6 Changes of MCF-7/Adr metabolic pathways (*left*) and overview of metabolites that were enriched in MCF-7/Adr cells (*right*). 1, 2 Aminoacyl-tRNA biosynthesis, 3 phenylalanine metabolism, 4 arginine and proline metabolism, 5 pantothenate and CoA biosynthesis, 6 butanoate metabolism, 7 citrate cycle (TCA cycle), 8 thiamine

metabolism, 9 alanine, aspartate, and glutamate metabolism, 10 cysteine and methionine metabolism, 11 phenylalanine, tyrosine, and tryptophan biosynthesis, 12 valine, leucine, and isoleucine biosynthesis, 13 beta-alanine metabolism, 14 propanoate metabolism

This interaction is mostly based on electrostatic interactions between positive ammonium groups of the polyamines and the negative phosphates of the polynucleic acids [36].

The intracellular antioxidative system was also an important factor in the protection of cells from chemical-induced

oxidative damage of DNA and cytotoxicity [37–39]. The antioxidative system mainly exhausted glutathione (GSH), which is a tripeptide containing sulfhydryl group (–SH) [40]. Glutathione also possessed high antioxidative activity and thus can eliminate superoxide anion free radicals and hydroxyl

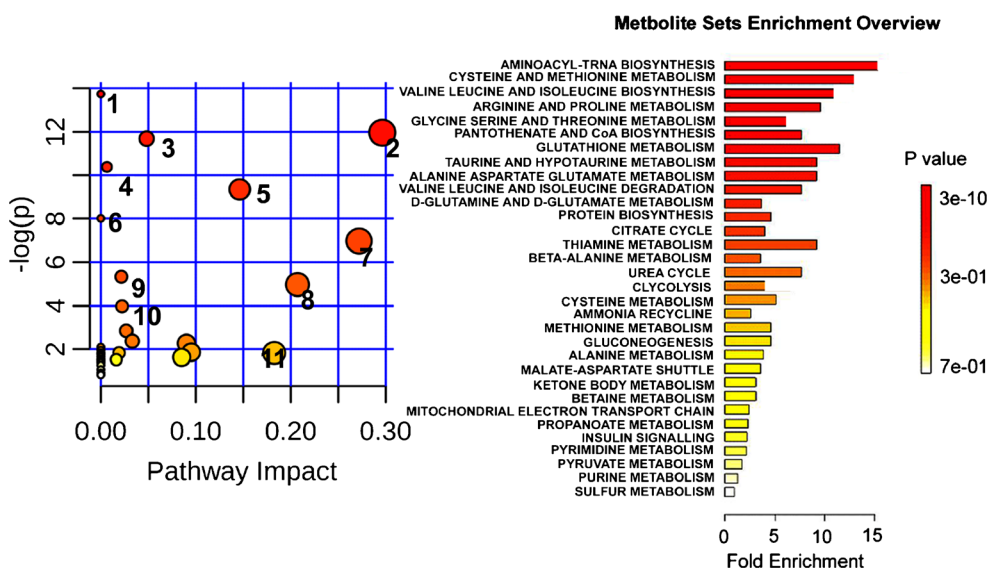


Fig. 7 Changes of COC1/DDP metabolic pathways (*left*) and overview of metabolites that were enriched in COC1/DDP cells (*right*). 1 Aminoacyl-tRNA biosynthesis, 2 cysteine and methionine metabolism, 3 valine, leucine, and isoleucine biosynthesis, 4 arginine and proline metabolism, 5 glycine, serine, and threonine metabolism, 6 pantothenate

and CoA biosynthesis, 7 glutathione metabolism, 8 taurine and hypotaurine metabolism, 9 alanine, aspartate, and glutamate metabolism, 10 valine, leucine, and isoleucine degradation, 11 D-glutamine and D-glutamate metabolism, 12 sulfur metabolism, 13 citrate cycle (TCA cycle), 14 thiamine metabolism, 15 beta-alanine metabolism

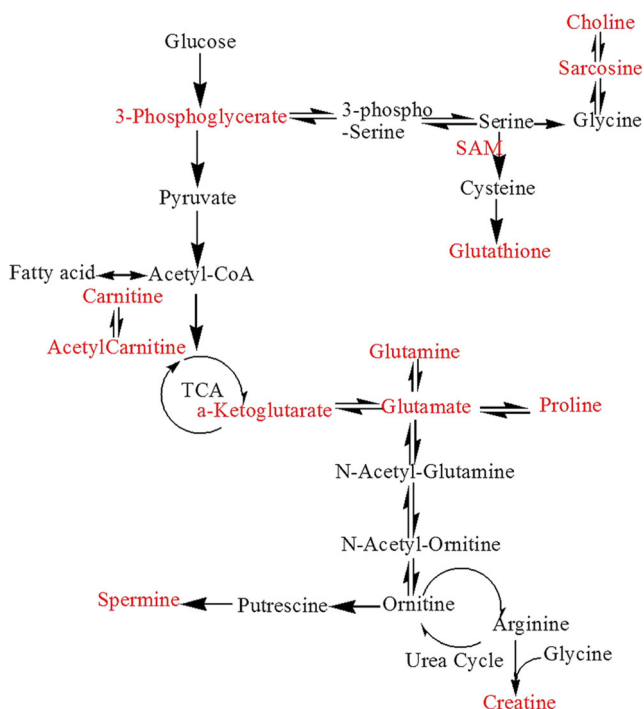


Fig. 8 Correlation metabolic pathways in response to MCF-7/Adr cells with multidrug resistance. The metabolites marked in red denote that they had been identified in the paper. The arrow direction denotes the metabolite's synthetic direction

free radicals. On the basis of this character, glutathione could promote the ability of cancer cells to survive under high oxidative stress, and also elevate the effect of drug resistance [41–43].

Conclusions

The use of metabolomics in exploring drug resistance is still a challenge in spite of some progresses being achieved. In this research, metabolomics analysis was performed in resistant cancer cells to understand the mechanisms of action. Comparison of the metabolites of cisplatin-resistant cells with the metabolites of doxorubicin-resistant cells revealed that some compounds are the same. The results indicate that drug resistance of cancer cell is related not only to the biosynthesis of proteins but also survival modes, such as antioxidation, the enhancement of energy metabolism, and accelerating the growth of cancer cells. The results also show that metabolomics can serve as an important tool in investigating the mechanisms of drug resistance by metabolic pathway analysis.

Acknowledgements This research was supported by the National Natural Science Foundation of China (No. 81373952, 81073040).

Compliance with ethical standards

Conflict of interest No potential conflicts of interest were disclosed.

References

- Eiermann W, Pienkowski T, Crown J, Sadeghi S, Martin M, Chan A, et al. Phase III study of doxorubicin/cyclophosphamide with concomitant versus sequential docetaxel as adjuvant treatment in patients with human epidermal growth factor receptor 2-normal, node-positive breast cancer: BCIRG-005 trial. *J Clin Oncol*. 2011;29:3877–84.
- Xu WH, Han M, Dong Q, Fu ZX, Diao YY, Liu H, et al. Doxorubicin-mediated radiosensitivity in multicellular spheroids from a lung cancer cell line is enhanced by composite micelle encapsulation. *Int J Nanomed*. 2012;7:2661–71.
- Orban E, Mezo G, Schlage P, Csik G, Kulic Z, Ansoerge P, et al. In vitro degradation and antitumor activity of oxime bond-linked daunorubicin-GnRH-III bioconjugates and DNA-binding properties of daunorubicin-amino acid metabolites. *Amino Acids*. 2011;41:469–83.
- Susa M, Iyer AK, Ryu K, Hornicek FJ, Mankin H, Amiji MM, et al. Doxorubicin loaded polymeric nanoparticulate delivery system to overcome drug resistance in osteosarcoma. *BMC Cancer*. 2009;9:399.
- Cao B, Li MJ, Zha WB, Zhao QJ, Gu RR, Liu LS, et al. Metabolomic approach to evaluating adriamycin pharmacodynamics and resistance in breast cancer cells. *Metabolomics*. 2013;9:960–73.
- Scheffer GL, Wijngaard PL, Flens MJ, Izquierdo MA, Slovak ML, Pinedo HM, et al. The drug-resistance-related protein LRP is the human major vault protein. *Nat Med*. 1995;1:578–82.
- Martin MB, Reiter R, Pham T, Avellanet YR, Camara J, Lahm M, et al. Estrogen-like activity of metals in MCF-7 breast cancer cells. *Endocrinology*. 2003;144:2425–36.
- Juliano R, Ling V, Graves J. Drug-resistant mutants of Chinese hamster ovary cells possess an altered cell surface carbohydrate component. *J Supramol Struct*. 1976;4:521–6.
- Alam J, Wicks C, Stewart D, Gong P, Touchard C, Otterbein S, et al. Mechanism of heme oxygenase-1 gene activation by cadmium in MCF-7 mammary epithelial cells role of p38 kinase and Nrf2 transcription factor. *J Biol Chem*. 2000;275:27694–702.
- Pogribny IP, Filkowski JN, Tryndyak VP, Golubov A, Shpyleva SI, Kovalchuk O. Alterations of microRNAs and their targets are associated with acquired resistance of MCF-7 breast cancer cells to cisplatin. *Int J Cancer*. 2010;127:1785–94.
- Hill SM, Blask DE. Effects of the pineal hormone melatonin on the proliferation and morphological characteristics of human breast cancer cells (MCF-7) in culture. *Cancer Res*. 1998;48:6121–6.
- Knowlden JM, Hutcheson IR, Jones HE, Madden T, Gee JM, Harper ME, et al. Elevated levels of epidermal growth factor receptor/c-erbB2 heterodimers mediate an autocrine growth regulatory pathway in tamoxifen-resistant MCF-7 cells. *Endocrinology*. 2003;144:1032–44.
- O'Connell K, Prencipe M, O'Neill A, Corcoran C, Rani S, Henry M, et al. The use of LC-MS to identify differentially expressed proteins in docetaxel-resistant prostate cancer cell lines. *Proteomics*. 2012;12:2115–26.
- Drabovich AP, Pavlou MP, Dimitromanolakis A, Diamandis EP. Quantitative analysis of energy metabolic pathways in MCF-7 breast cancer cells by selected reaction monitoring assay. *Mol Cell Proteomics*. 2012;11:422–34.
- Kovalchuk O, Filkowski J, Meservy J, Ilnytskyy Y, Tryndyak VP, Chekhun CF, et al. Involvement of microRNA-451 in resistance of the MCF-7 breast cancer cells to chemotherapeutic drug doxorubicin. *Mol Cancer Ther*. 2008;7:2152–9.
- Lutz NW, Franks SE, Frank MH, Pomer S, Hull WE. Investigation of multidrug resistance in cultured human renal cell carcinoma cells

- by 31P-NMR spectroscopy and treatment survival assays. *Magma*. 2005;18:144–61.
17. Klawitter J, Kominsky DJ, Brown JL, Klawitter J, Christians U, Leibfritz D, et al. Metabolic characteristics of imatinib resistance in chronic myeloid leukaemia cells. *Br J Pharmacol*. 2009;158:588–600.
 18. Dewar BJ, Keshari K, Jeffries R, Dzeja P, Graves LM, Macdonald JM. Metabolic assessment of a novel chronic myelogenous leukemic cell line and an imatinib resistant subline by H NMR spectroscopy. *Metabolomics*. 2010;6:439–50.
 19. Hirschhaeuser F, Sattler UG, Mueller-Klieser W. Lactate: a metabolic key player in cancer. *Cancer Res*. 2011;71:6921–5.
 20. Wu G, Fang Y-Z, Yang S, Lupton JR, Turner ND. Glutathione metabolism and its implications for health. *J Nutr*. 2004;134:489–92.
 21. Munoz-Pinedo C, El Mjyyad N, Ricci JE. Cancer metabolism: current perspectives and future directions. *Cell Death Dis*. 2012;3, e248.
 22. Berg M, Vanaerschot M, Jankevics A, Cuypers B, Maes I, Mukherjee S, et al. Metabolic adaptations of *Leishmania donovani* in relation to differentiation, drug resistance, and drug pressure. *Mol Microbiol*. 2013;90:428–42.
 23. Canuto GA, Castilho-Martins EA, Tavares M, Lopez-Gonzalvez A, Rivas L, Barbás C. CE-ESI-MS metabolic fingerprinting of *Leishmania* resistance to antimony treatment. *Electrophoresis*. 2012;33:1901–10.
 24. Antti H, Fahlgren A, Nasstrom E, Kouremenos K, Sunden-Cullberg J, Guo Y, et al. Metabolic profiling for detection of *Staphylococcus aureus* infection and antibiotic resistance. *PLoS One*. 2013;8, e56971.
 25. Halama A, Moller G, Adamski J. Metabolic signatures in apoptotic human cancer cell lines. *OMICS*. 2011;15:325–35.
 26. Zhao YY, Lei P, Chen DQ, Feng YL, Bai X. Renal metabolic profiling of early renal injury and renoprotective effects of *Poria cocos* epidermis using UPLC Q-TOF/HSMS/MSE. *J Pharm Biomed*. 2013;81-82:202-9.
 27. Tedeschi P, Markert E, Gounder M, Lin H, Dvorzhinski D, Dolfi S, et al. Metabolic profiling for detection of *Staphylococcus aureus* infection and antibiotic resistance. *Cell Death Dis*. 2013;4, e877.
 28. Caso G, McNurlan MA, McMillan ND, Eremin O, Garlick PJ. Tumour cell growth in culture: dependence on arginine. *Clin Sci*. 2004;107:371–9.
 29. Brune DC, Hampton B, Kobayashi R, Leone JW, Linse KD, Pohl J, et al. ABRF ESRG 2006 study: Edman sequencing as a method for polypeptide quantitation. *J Biomol Tech*. 2007;18:306–20.
 30. Brune K. Persistence of NSAIDs at effect sites and rapid disappearance from side-effect compartments contributes to tolerability. *Curr Med Res Opin*. 2007;23:2985–95.
 31. Kalac P. Health effects and occurrence of dietary polyamines: a review for the period 2005-mid 2013. *Food Chem*. 2014;161:27–39.
 32. Brzozowski T, Konturek PC, Konturek SJ, Brzozowska I, Kwiecien S, Hahn EG. Involvement of ornithine decarboxylase and polyamines in epidermal growth factor-induced recovery of gastric mucosa from gastric lesions provoked by stress. *Regul Pept*. 1998;74: 73–84.
 33. Ernestus RI, Rohn G, Schroder R, Els T, Klekner A, Paschen W, et al. Polyamine metabolism in brain tumours: diagnostic relevance of quantitative biochemistry. *J Neurol Neurosurg Psychiatry*. 2001;71: 88–92.
 34. Ekegren T, Gomes-Trolin C. Determination of polyamines in human tissues by precolumn derivatization with 9-fluorenylmethyl chloroformate and high-performance liquid chromatography. *Anal Biochem*. 2005;338:179–85.
 35. Vuckovic D. Current trends and challenges in sample preparation for global metabolomics using liquid chromatography-mass spectrometry. *Anal Bioanal Chem*. 2012;403:1523–48.
 36. Yao X, Lu C-D. Functional characterization of the potRABCD operon for spermine and spermidine uptake and regulation in *Staphylococcus aureus*. *Curr Microbiol*. 2014;69:75–81.
 37. Xu L, Zhang XZ, Guo Y, Ren Q, Wu XX. Preparation and anti-oxidative effects of corn peptides. *Chem Res Chin Univ*. 2002;18: 299–302.
 38. Chen YP, Zhang J, Yang ZJ, Yu F, Li YQ. Relationship between nitric oxide accumulation, anti-oxidative system and freezing tolerance in the leaves of sabinia during cold adaptation. *J Anim Plant Sci*. 2012;22:1133–41.
 39. Swiderska-Kolacz G, Klusek J, Kolataj A. The effect of exogenous GSH, GSSG and GST-E on glutathione concentration and activity of selected glutathione enzymes in the liver, kidney and muscle of mice. *Anim Sci Pap Rep*. 2007;25:111–7.
 40. Powis G. Anticancer drugs acting against signaling pathways. *Curr Opin Oncol*. 1995;7:554–9.
 41. Pastore A, Federici G, Bertini E, Piemonte F. Analysis of glutathione: implication in redox and detoxification. *Clin Chim Acta*. 2003;333:19–39.
 42. Dringen R, Pfeiffer B, Hamprecht B. Synthesis of the antioxidant glutathione in neurons: supply by astrocytes of CysGly as precursor for neuronal glutathione. *J Neurosci*. 1999;19:562–9.
 43. Cullen KV, Davey RA, Davey MW. Verapamil-stimulated glutathione transport by the multidrug resistance-associated protein (MRP1) in leukaemia cells. *Biochem Pharmacol*. 2001;62:417–24.